



Enhanced sensing performance of catalytic combustion methane sensor by using Pd nanorod/ γ -Al₂O₃

Fengmin Liu, Yiqun Zhang, Yingshuo Yu, Jing Xu, Jianbo Sun, Geyu Lu*

State Key Laboratory on Integrated Optoelectronics, College of Electronic Science and Engineering, Jilin University, 2699 Qianjin Street, Changchun 130012, China

ARTICLE INFO

Article history:

Received 28 March 2011
Received in revised form 23 August 2011
Accepted 12 September 2011
Available online 17 September 2011

Keywords:

Pd
Dispersion state
Gas sensor
Methane

ABSTRACT

Novel metal palladium was loaded on γ -Al₂O₃ using decompression distillation, ultrasonic impregnation, and isometric impregnation. Of these loading methods, isometric impregnation was examined to be the best method for preparing high-performance Pd/Al₂O₃ catalysts. The observation with transmission electron microscopy demonstrated that Pd nanorods were formed on γ -Al₂O₃ for the samples preparing with isometric impregnation. The correlation of the morphology of Pd with the loading time was also investigated: Pd catalysts loaded for 2 and 6 h had the almost same nanorod morphology and relatively uniform size. Nitrogen adsorption and desorption isotherms indicate that Pd nanorods increased the BET-specific surface area of Pd/ γ -Al₂O₃. The catalytic combustion gas sensor prepared using Pd/ γ -Al₂O₃ via isometric impregnation exhibited high sensitivity to methane as well as fast response and recovery properties.

© 2011 Elsevier B.V. All rights reserved.

1. Introduction

Methane is a natural gas widely used in industrial and domestic applications. As its leakage results in explosions and fires, with that in coal being particularly disastrous and fatal, the gas alarm or systems monitoring methane concentrations are therefore urgently necessary. Highly sensitive and stable methane sensor is the most important device for constructing high-performance alarm systems. Several types of methane sensors have been developed [1–7], such as the resistive sensor using SnO₂, the optical sensor based on infrared absorption and the catalyst combustion sensor. Of these types, the catalytic combustion methane sensor has been widely applied for detecting methane in residences and coal mines because of its simple structure, low cost, good stability and anti-poisoning properties. Recent developments of the catalytic combustion methane sensor have focused on the preparation of Pd/Al₂O₃, such as the preparation method [8–10] of Al₂O₃ support, particle size [11–14] and oxidation [15,16] of Pd catalyst and Pd precursor and solvent for loading [17,18,10,19,28], as well as the design of microhotplate [29]. However, lower sensitivity of the reported catalytic combustion methane sensor using Pd/Al₂O₃ limited its utility to monitor the lower concentration methane gas [30–33]. Some examples of previous works about the catalytic gas sensors are shown in Table 1.

In recent years, nanoscience has received growing interest due to the unique chemical and physical properties of nanomaterials. These properties are closely related to morphology, which in turn is affected by synthesized conditions. For example, different ZnO morphologies, nanoparticles, nanowires, nanorods, and nanoflowers show distinct properties [20–26]. Although Pd/Al₂O₃ materials have already been used for the catalytic combustion of methane, only Pd nanoparticles have been reported as the nanostructures dispersing on Al₂O₃ support.

In this work, decompression distillation, ultrasonic impregnation and isometric impregnation were applied to load Pd catalysts on γ -Al₂O₃. The effects of these loading processes and conditions on the morphology, dispersion state of Pd on γ -Al₂O₃ and the corresponding sensing properties of the catalytic combustion methane sensors were specifically investigated.

2. Experimental

2.1. Preparation of γ -Al₂O₃ support and loading of Pd catalyst

γ -Al₂O₃ was prepared by sintering commercial Al₂O₃·H₂O (321-25785 Boehmite, Wako) at 750 °C for 6 h. Pd catalyst was loaded on the as-prepared γ -Al₂O₃ with decompression distillation, ultrasonic impregnation and isometric impregnation. For decompression distillation, 0.2 g γ -Al₂O₃ and 0.353 mL Pd(NO₃)₂ solution (Shanghai Jiuyue Chemical Co., Ltd.) were mixed inside a flask under stirring at 50 °C; deionized water was then added into the flask until the solution volume reached 50 mL. The sample was collected after the water completely evaporated. In ultrasonic

* Corresponding author. Tel.: +86 431 85167808; fax: +86 431 85167808.
E-mail address: luyg@jlu.edu.cn (G. Lu).

Table 1
Examples of previous works about the catalytic gas sensors.

Catalyst	Constant voltage	Sensitivity (mV/% CH ₄)	Reference
Pd/Pt/Al ₂ O ₃	1.3	2	[29]
Pd/Pb/Al ₂ O ₃	2.5 ± 0.1	22–29	[32]
Pd/Pb/CeO ₂	2.5 ± 0.1	24–32	[32]
Pd/Al ₂ O ₃	–	20–25	[33]
PdO/Al ₂ O ₃	–	17–21	[33]

impregnation, 0.2 g γ -Al₂O₃ and a required amount of Pd(NO₃)₂ solution were ultrasonically mixed in a beaker at 40 kHz for 2 h. For isometric impregnation, the maximum volume of Pd(NO₃)₂ solution absorbed by γ -Al₂O₃ powder was dropped into γ -Al₂O₃ at room temperature and steeped for 2, 6, and 10 h. Finally, the precursors of Pd (15 wt%)/ γ -Al₂O₃ prepared with these three processes were dried at 80 °C for 1 h and subsequently reduced under a mixed atmosphere with 5% H₂ in N₂ at 290 °C for 2 h.

2.2. Characterization of Pd/ γ -Al₂O₃

X-ray diffraction (XRD, Rigaku wide-angle X-ray diffraction D/max rA, using Cu K α radiation at wavelength $\lambda = 0.1541$ nm) was carried out to analyze the structure of Al₂O₃ support and identify the formation of pure metal Pd. The BET-specific surface areas of the samples were measured by nitrogen adsorption measurements (Gemini VII 2390). The as-reduced Pd (15 wt%)/ γ -Al₂O₃ catalyst was further characterized by transmission electron microscopy (TEM, HITACHI H-8100) to determine the morphology and dispersion of Pd on γ -Al₂O₃.

2.3. Fabrication and measurement of the sensors

The sensing and reference elements were fabricated by coating the obtained Pd/ γ -Al₂O₃ and γ -Al₂O₃, respectively, onto platinum coils, and then sintered at 600 °C for 2 h. The obtained two elements (resistances of the Pt coils are about 3.5 Ω at room temperature) were combined with two constant resistances (2 k Ω) for constructing a Wheatstone bridge (Fig. 1). In order to keep the sensing and reference devices at 450 °C, 2.5 V of voltage was applied between the two devices. The output (U_0) of the catalytic combustion methane sensor was formulated with the voltage between the middle points of the two branches of Wheatstone bridge. The response is the difference of the outputs in air and methane. And the sensitivity of the sensor is defined as the slope of

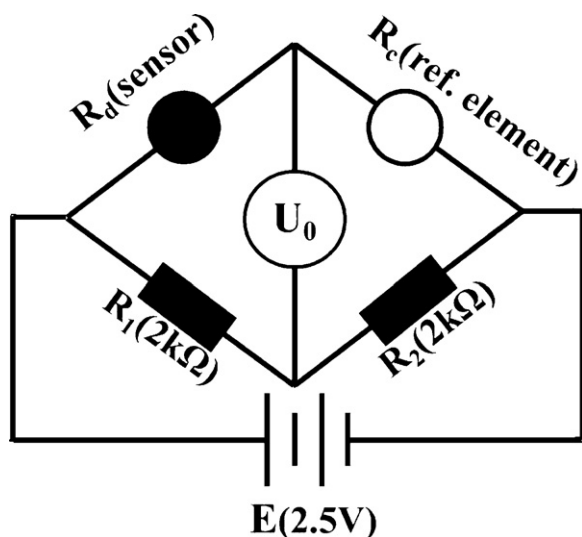


Fig. 1. Testing circuit of the catalytic combustion type sensor.

Table 2
Pd grain sizes of Pd/ γ -Al₂O₃ obtained under different conditions.

Loading method	Pd grain size (nm)
Decompression distillation	30.43
Ultrasonic impregnation	22.74
Isometric impregnation	
0 h	8.19
2 h	8.75
6 h	9.16
10 h	9.91

the dependence of output (voltage) on the gas concentration. The sensor was evaluated with a static process: the sensors attached with the measuring circuits were put into a closed chamber, and a given amount of methane was injected into the chamber and the outputs of the sensors were measured by a digital multimeter.

When the sensor kept at 450 °C was exposed to methane diluted with air, the following combustion reaction took place on the surface of Pd/ γ -Al₂O₃. The combustion heat was transferred to the Pt coil coated by Pd/ γ -Al₂O₃, and then the resistance of the Pt coil increased.



On the other hand, for the reference element, the above combustion reaction could not proceed on the surface of pure γ -Al₂O₃, and the resistance of the reference element kept a constant. Therefore, the output of the sensor in methane could be expressed as following:

$$U_0 = \frac{R_d + \Delta R_d}{R_c + (R_d + \Delta R_d)} E - \frac{E}{2} \quad (2)$$

Here, R_d is the resistance of sensing element in air, ΔR_d represents the difference of the resistances in methane and air for sensing element, R_c is the resistance of the reference element in air or methane, E is the voltage applied in the sensor branch. Because ΔR_d is far less than R_d , and R_c is almost same as R_d ($R_d \approx R_c = R$), the expression (2) can be simplified to (3):

$$U_0 = \frac{E}{R_c + R_d} \Delta R_d = \frac{E}{2R} \Delta R_d = K \Delta R_d, \quad \left(K = \frac{E}{2R} \right) \quad (3)$$

ΔR_d can be described with the following expression:

$$\Delta R_d = \rho \cdot \Delta T = \rho \cdot \frac{Q}{C} = \rho \cdot \alpha \cdot m \cdot \frac{\Delta H}{C} \quad (4)$$

Here, ρ is the resistance temperature constant, ΔT is the change of the temperature of the sensing element, Q represents the heat produced the combustion reaction on Pd/ γ -Al₂O₃, C is the heat capacity of the sensing element, m is the methane concentration, ΔH is combustion heat, and α stands for a constant. From the expression (4), we could obtain expression (5) by combining (3) with (4).

$$U_0 = \beta \cdot m \quad (5)$$

Here, $\beta = K \cdot \rho \cdot \alpha \cdot \Delta H / C$. Therefore, the output is linear with the concentration of methane.

3. Results and discussion

3.1. Characterization of Pd/ γ -Al₂O₃ and γ -Al₂O₃

Fig. 2 gives the XRD data of Al₂O₃ prepared by sintering boehmite at 750 °C for 6 h, and the obtained sample was testified to pure γ -Al₂O₃. The XRD of Pd/ γ -Al₂O₃ obtained by three kinds of loading methods and with different loading times is shown in Figs. 2 and 3, which identify the formation of Pd. The Pd grain sizes of these samples are further calculated using Scherrer equation, shown in Table 2. Among these three loading methods, the

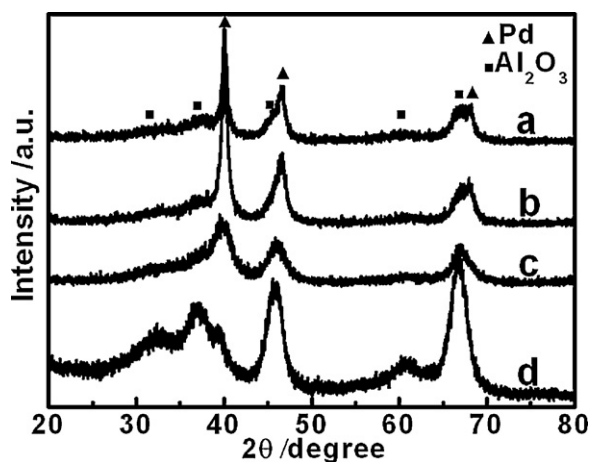


Fig. 2. XRD pattern of Al₂O₃ prepared by sintering the commercial Al₂O₃·H₂O (d) and Pd/γ-Al₂O₃ obtained by decompression distillation (a), ultrasonic impregnation (b) and isometric impregnation (c).

samples prepared by isometric impregnation gave the smallest Pd grain sizes (≤ 10 nm). This is reasonable because the loading temperatures in isometric impregnation is lower than that in decompression distillation and ultrasonic impregnation, so the growth rate of Pd nucleation are initially uniform which inhibits further growth [34].

Fig. 4 shows N₂ adsorption–desorption isotherms and the corresponding pore size distribution curve of γ-Al₂O₃. The characteristic type IV shape means that the γ-Al₂O₃ is porous. The pore size distributes in a narrow range, indicating the pore size is uniform and most of them is at 11.21 nm. So Pd particles prepared with isometric impregnation could enter into the channels of γ-Al₂O₃.

The BET-specific surface areas of the as-prepared samples are shown in Table 3. The samples prepared by isometric impregnation gave the largest specific surface areas among the three loading methods. Loading processes have two subprocesses: the transport of Pd²⁺ into γ-Al₂O₃ and the hydrolysis of Pd²⁺ on γ-Al₂O₃. Compared with isometric impregnation, decompression distillation and ultrasonic impregnation have much greater water volumes and much lower Pd concentrations, thereby slowing down the loading speed. Moreover, heat occurs during decompression distillation and ultrasonic impregnation. Hence, the hydrolysis of Pd²⁺ on γ-Al₂O₃ is dominant and the Pd dispersion is less uniform under decompression distillation and ultrasonic impregnation.

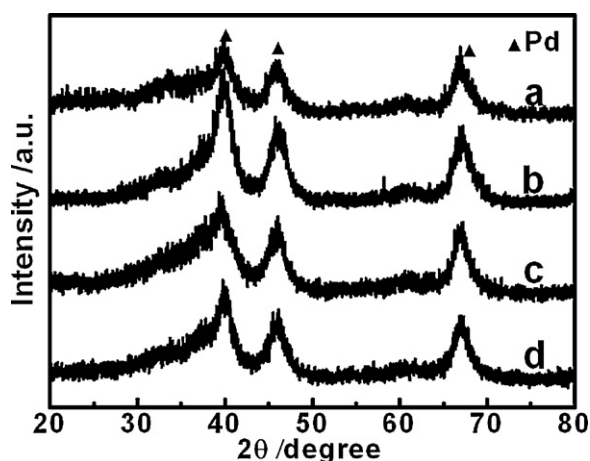


Fig. 3. XRD pattern of Pd/γ-Al₂O₃ obtained under different impregnation times (a) 0 h, (b) 2 h, (c) 6 h and (d) 10 h.

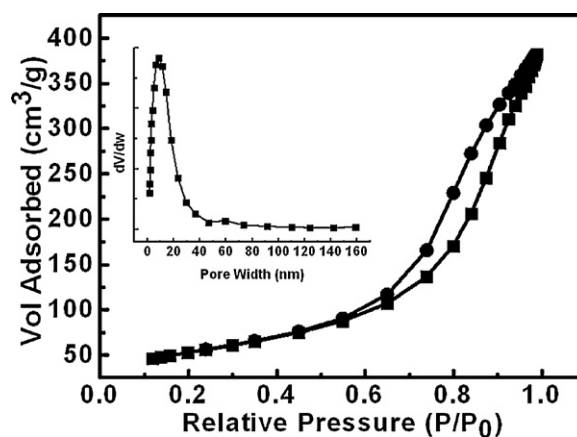


Fig. 4. N₂ adsorption–desorption isotherms and the corresponding pore size distribution curve for γ-Al₂O₃.

Fig. 5 shows the TEM images and the Pd distribution of Pd/γ-Al₂O₃ obtained from the three Pd loading methods, the black spots on TEM images is Pd. The largest Pd aggregations on γ-Al₂O₃ occurred in decompression distillation, whereas Pd dispersion improved, to some extent, under ultrasonic impregnation. The best Pd dispersion was achieved by isometric impregnation, in which the Pd showed a uniform nanorod structure. The oriented attachment mechanism [27] can explain the Pd nanorod formation in γ-Al₂O₃: Pd particles moderately enter the many channels that exist inside γ-Al₂O₃ and the hydrolysis of Pd²⁺ on γ-Al₂O₃ are balanced. When Pd particles nucleate side by side on the same channel, these adjacent particles will spontaneously self-organize to share a common crystallographic orientation during growth and form a nanorod single crystal response to the channel structure. The Pd crystal size distributions are also shown in Fig. 5b, d, and f. The average size of the Pd obtained by decompression distillation and ultrasonic impregnation has a broad size distribution, the average crystal size of the Pd determined from Fig. 5b and d is 30 nm and 20 nm, respectively. For isometric impregnation, the Pd nanorod sizes are relatively uniform, and the average diameter of the Pd nanorod determined from Fig. 5f is 8 nm. These results are consonant with the average grain size estimated from the XRD analysis.

Fig. 6 shows the TEM images and the Pd distribution of Pd/γ-Al₂O₃ obtained by isometric impregnation with different loading times. The Pd structures on γ-Al₂O₃ are evidently altered by the increase in impregnation time. At 0 h of impregnation, the Pd structure was a mixture of nanoparticles and nanorods and the average grain size of the Pd is about 10 nm. At 2 and 6 h, the Pd nanoparticles disappeared and the Pd structure was clearly composed of uniform nanorods, and the Pd diameter is about 8 nm. But at 10 h, the Pd structure was a mixture of large nanoparticles and nanorods and the grain size of the Pd is over 10 nm. BET-specific surface areas

Table 3
BET-specific surface areas of Pd/γ-Al₂O₃ obtained under different conditions.

Loading method	Specific surface area (m ² g ⁻¹)
Decompression distillation	142.7
Ultrasonic impregnation	159.9
Isometric impregnation	
0 h	164.9
2 h	175.1
6 h	176.3
10 h	166.8

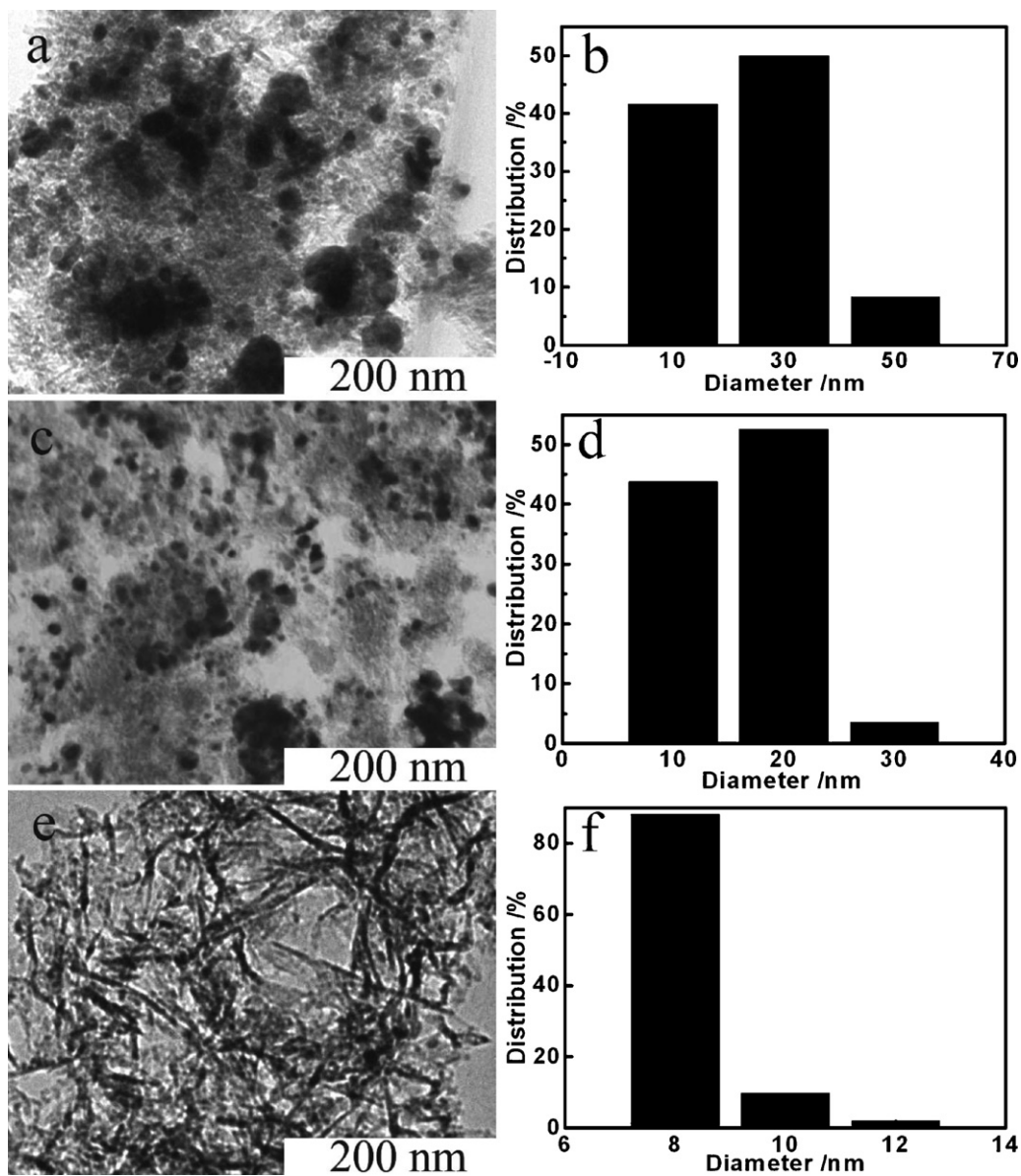


Fig. 5. TEM images of Pd/ γ -Al₂O₃ obtained by decomposition distillation (a), ultrasonic impregnation (c) and isometric impregnation (e) and the corresponding Pd distribution of Pd/ γ -Al₂O₃ (b, d and f).

were the largest or smallest for uniform nanorods or nanoparticles (Table 3). The Pd dispersion states were strongly affected by both the transport of Pd²⁺ into γ -Al₂O₃ and the hydrolysis of Pd²⁺ on γ -Al₂O₃. The reaction pathways are shown in Fig. 7. The γ -Al₂O₃ channels play important roles as templates to the formation of Pd nanorods. The transport of Pd²⁺ into γ -Al₂O₃ was dominant when the impregnation time was short. At 0 h of impregnation (Fig. 7a), a little amount of Pd on γ -Al₂O₃ became nanorods, but much of the remaining Pd did not enter the channel of Al₂O₃ and turn into nanoparticles. However, for 2 and 6 h of impregnation (Fig. 7b), Pd completely moved into Al₂O₃ and became uniform Pd nanorods. Beyond 6 h of impregnation, in the first stage of loading process, the formation of Pd nanorods is dominant, with the increasing of the loading time, the particles constructing nanorods become larger, and some particles departed from the nanorods and exited separately. Hence, up to 10 h of impregnation (Fig. 7c), the Pd structure on Al₂O₃ was a mixture of nanoparticles and nanorods.

3.2. Sensing properties of Pd/ γ -Al₂O₃ to methane

Fig. 8 shows the dependence of the response on the methane concentration for the catalytic combustion sensors using the Pd/ γ -Al₂O₃ obtained by decomposition distillation, ultrasonic impregnation and isometric impregnation. The Pd/ γ -Al₂O₃ obtained with isometric impregnation gave the highest sensitivity to methane. The sensitivity of Pd/ γ -Al₂O₃ obtained with isometric impregnation was as high as 34 mV/%CH₄, which is about twice that of Pd/ γ -Al₂O₃ obtained by decomposition distillation. The results show that the loading method significantly influences the sensing properties of Pd/ γ -Al₂O₃ to methane.

Fig. 9 shows the correlation between sensitivity of the methane sensors based on the Pd/ γ -Al₂O₃ obtained by isometric impregnation and Pd loading times. The sensitivity of the sensor was higher at 2 and 6 h of impregnation, during which the Pd nanostructure formed was that of uniform nanorods. The sensitivity was lower at 0 and 10 h of loading, during which a mixture of nanoparticles and

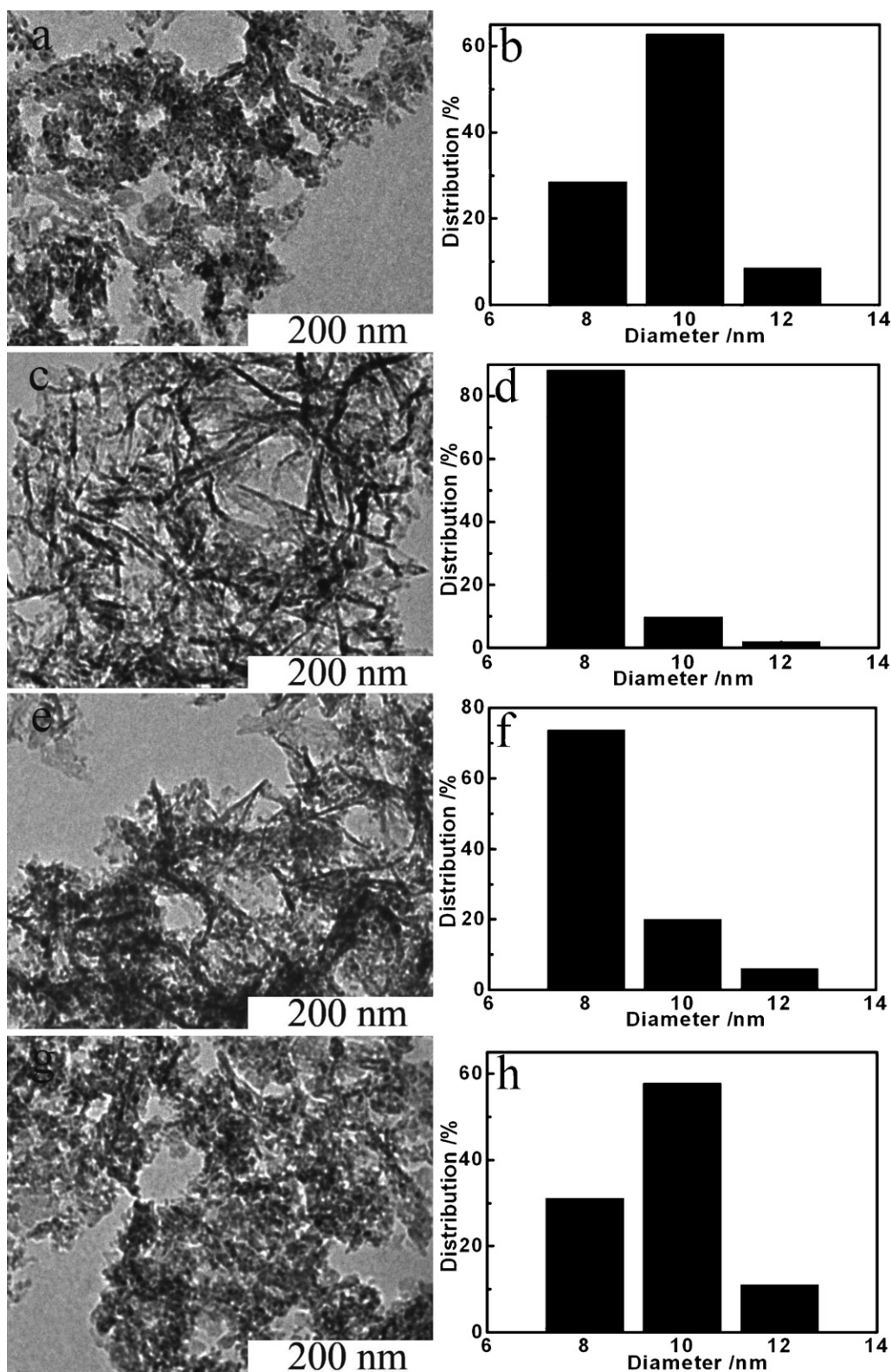


Fig. 6. TEM images of Pd/ γ -Al₂O₃ obtained under different impregnation times (a) 0 h, (c) 2 h, (e) 6 h and (g) 10 h and the corresponding Pd distribution of Pd/ γ -Al₂O₃ (b, d, f and h).

nanorods formed. These further illustrate that the sensitivity of the Pd/ γ -Al₂O₃ material is closely related to the morphology of Pd.

The catalytic combustion sensor is not selective, but its response depends on the kind and concentration of the flammable gas, combustion heat, the diffusion rate of the flammable gas in the sensor

and the conduction [30]. Various gases of different concentrations, including 3000 ppm CH₄, 100 ppm CO, 1000 ppm H₂, 30 ppm H₂S, 500 ppm C₄H₁₀, were tested according to the working environment (Fig. 10). The sensors are almost responseless to CO and H₂S, but C₄H₁₀ and H₂ exert some interfere to the sensors for testing

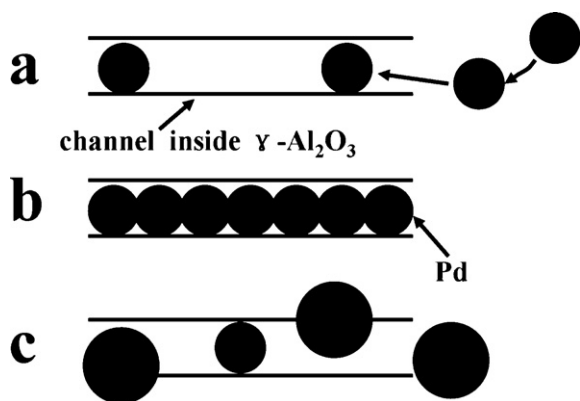


Fig. 7. Pd nanorods reaction pathways, earlier stage (a), interim stage (b) and later stage (c).

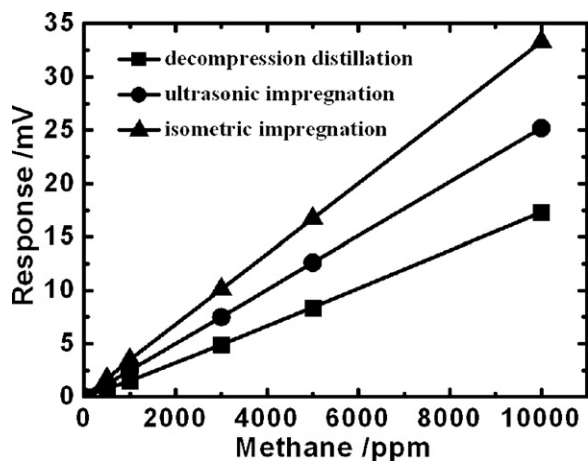


Fig. 8. Response of the sensors fabricated through different Pd loading methods.

methane. Even so, the sensor using Pd/γ-Al₂O₃ prepared with isometric impregnation still gives the high response to methane.

The response and recovery curves of the catalytic combustion sensors based on the Pd/γ-Al₂O₃ obtained by decomposition distillation, ultrasonic impregnation and isometric impregnation to 3000 ppm CH₄ are shown in Fig. 11a–c, respectively. Although all the sensors using different Pd/γ-Al₂O₃ catalysts display quick response and recovery speeds to methane, the repeatability is obviously different. The outputs both in air and 3000 ppm methane for

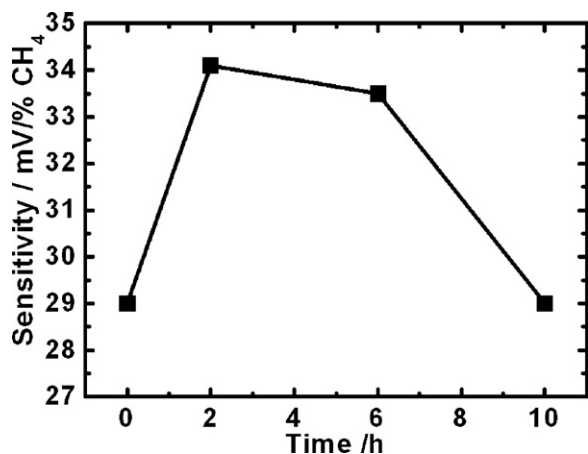


Fig. 9. Correlation between loading time during isometric impregnation and sensitivity of the methane sensor.

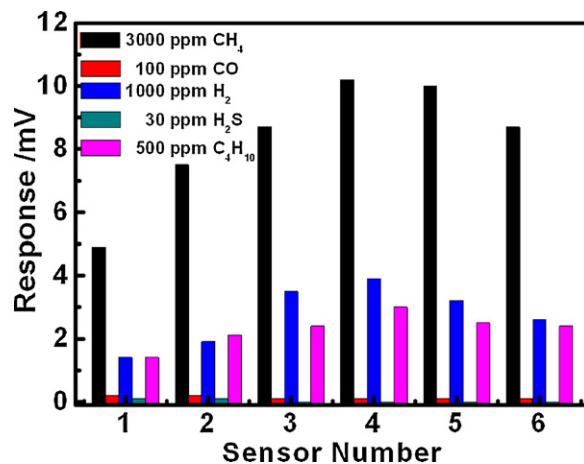


Fig. 10. Selectivity of the sensors to various gases of different concentrations.

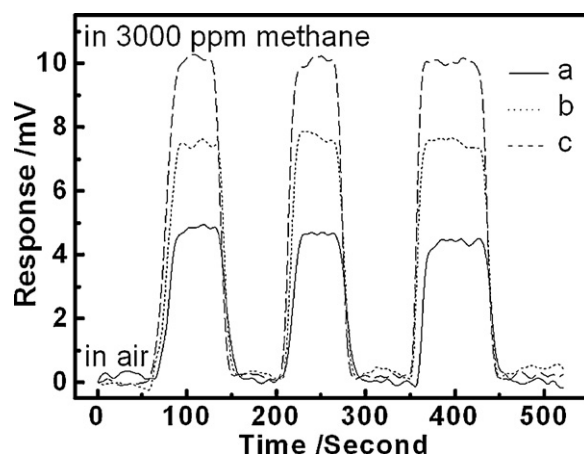


Fig. 11. The response and recovery curves of the catalytic combustion sensors fabricated with decomposition distillation (a), ultrasonic impregnation (b) and isometric impregnation (c).

the sensors based on Pd/γ-Al₂O₃ prepared by decomposition distillation (Fig. 11a) are downwards after three cycles. At the same time, Fig. 11b exhibits that the sensors' output in 3000 ppm methane is stable, but the one in air is upward. Fig. 11c shows that the outputs in air and 3000 ppm methane are repeatable for the sensors

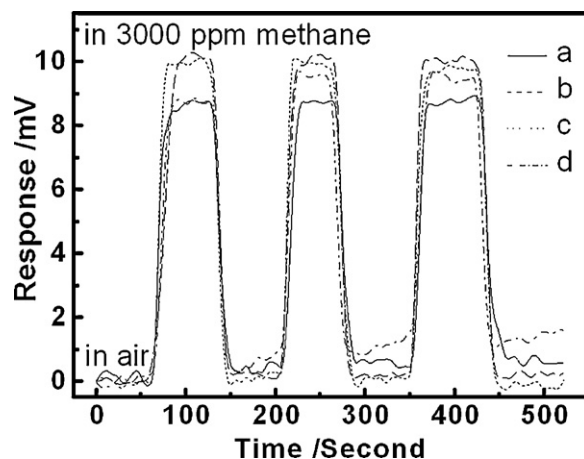


Fig. 12. Correlation between loading time during isometric impregnation and response and recovery curves of the methane sensor. (a) 0 h, (b) 2 h, (c) 6 h and (d) 10 h.

using Pd/ γ -Al₂O₃ from isometric impregnation. Fig. 12 shows the response and recovery curves of the methane sensors based on the Pd/ γ -Al₂O₃ material obtained by isometric impregnation with different Pd loading times. It can be seen from Fig. 12 that the outputs of the sensors using Pd/ γ -Al₂O₃ by isometric impregnation for 2 and 6 h are more stable than those for 0 and 10 h. Above results indicated that Pd nanorods sensors using the catalyst via isometric impregnation for 2 and 6 h not only exhibit higher response, but also have better repeatability than those using catalysts with decompression distillation, ultrasonic impregnation.

4. Conclusions

Pd morphology is an important factor affecting the sensing performance of the catalytic combustion sensors. Different Pd loading methods result in distinct Pd morphologies, thereby affecting the sensing performance of sensors. Of the three loading methods described in this study, isometric impregnation gave the highest sensitivity as well as the most rapid response and recovery rates. Moreover, at 2 and 6 h of loading, the Pd nanostructure was the uniform nanorods and the Pd/ γ -Al₂O₃ catalyst had the largest specific surface area, the highest sensitivity and the most rapid response and recovery rates to methane, indicating that the morphology of Pd is closely related to loading time in the isometric impregnation method. Compared to previous works about the catalytic gas sensors, this sensor obtained by isometric impregnation with 2 h performed high sensitivity to methane as well as fast response and recovery properties.

Acknowledgement

This work was supported by the National Science Fund (No. 60906036, No. 61074172).

References

- [1] K. Persson, A. Ersson, K. Jansson, J.L.G. Fierro, S.G. Jaras, Influence of molar ratio on Pd-Pt catalysts for methane combustion, *J. Catal.* 243 (2006) 14–24.
- [2] J.M. Jones, V.A. Dupont, R. Brydson, D.J. Fullerton, N.S. Nasri, A.B. Ross, A.V.K. Westwood, Sulphur poisoning and regeneration of precious metal catalysed methane combustion, *Catal. Today* 81 (2003) 589–601.
- [3] B.K. Min, S.D. Choi, Undoped and 0.1 wt.% Ca-doped Pt-catalyzed SnO₂ sensors for CH₄ detection, *Sens. Actuators B: Chem.* 108 (2005) 119–124.
- [4] K. Chatterjee, S. Chatterjee, A. Banerjee, M. Raut, N.C. Pal, A. Sen, H.S. Maiti, The effect of palladium incorporation on methane sensitivity of antimony doped tin dioxide, *Mater. Chem. Phys.* 81 (2003) 33–38.
- [5] Y.J. Lu, J. Li, J. Han, H.-T. Ng, C. Binder, C. Partridge, M. Meyyappan, Room temperature methane detection using palladium loaded single-walled carbon nanotube sensors, *Chem. Phys. Lett.* 391 (2004) 344–348.
- [6] M. Saha, A. Banerjee, A.K. Halder, J. Mondal, A. Sen, H.S. Maiti, Effect of alumina addition on methane sensitivity of tin dioxide thick films, *Sens. Actuators B: Chem.* 79 (2001) 192–195.
- [7] F. Quaranta, R. Rella, P. Siciliano, S. Capone, M. Epifani, L. Vasanelli, A. Licciulli, A. Zocco, A novel gas sensor based on SnO₂/Os thin film for the detection of methane at low temperature, *Sens. Actuators B: Chem.* 58 (1999) 350–355.
- [8] J.V. Kumar, N. Lingaiah, K.S.R. Rao, S.P. Ramnani, S. Sabharwal, P.S.S. Prasad, Investigation of palladium species in Pd/Al₂O₃ catalysts prepared by radiolysis method, *Catal. Commun.* 10 (2009) 1149–1152.
- [9] R.J.H. Grisel, P.J. Kooyman, B.E. Nieuwenhuys, Influence of the preparation of Au/Al₂O₃ on CH₄ oxidation activity, *J. Catal.* 191 (2000) 430–437.
- [10] G.Q. Guan, K. Kusakabe, M. Tameda, M. Uehara, H. Maeda, Catalytic combustion of methane over Pd-based catalyst supported on a macroporous alumina layer in a microchannel reactor, *Chem. Eng. J.* 144 (2008) 270–276.
- [11] C.A. Muller, M. Maciejewski, R.A. Koepfel, A. Baiker, Combustion of methane over palladium/zirconia derived from a glassy Pd–Zr alloy: effect of Pd particle size on catalytic behavior, *J. Catal.* 166 (1997) 36–43.
- [12] R.F. Hicks, H. Qi, M.L. Young, R.G. Lee, Structure sensitivity of methane oxidation over platinum and palladium, *J. Catal.* 122 (1990) 280–294.
- [13] R.F. Hicks, H. Qi, M.L. Young, R.G. Lee, Effect of catalyst structure on methane oxidation over palladium on alumina, *J. Catal.* 122 (1990) 295–306.
- [14] C.A. Muller, M. Maciejewski, R.A. Koepfel, A. Baiker, Combustion of methane over palladium/zirconia: effect of Pd-particle size and role of lattice oxygen, *Catal. Today* 47 (1999) 245–252.
- [15] R. Burch, P.K. Loader, Investigation of Pt/Al₂O₃ and Pd/Al₂O₃ catalysts for the combustion of methane at low concentrations, *Appl. Catal. B: Environ.* 5 (1994) 149–164.
- [16] L.M.T. Simplicio, S.T. Brandao, E.A. Sales, L. Lietti, F.B. Verduraz, Methane combustion over PdO-alumina catalysts: the effect of palladium precursors, *Appl. Catal. B: Environ.* 63 (2006) 9–14.
- [17] N.M. Kinnunen, M. Suvanto, M.A. Moreno, A. Savimaki, K. Kallinen, T.-J.J. Kinnunen, T.A. Pakkanen, Methane oxidation on alumina supported palladium catalysts: effect of Pd precursor and solvent, *Appl. Catal. A: Gen.* 370 (2009) 78–87.
- [18] P.O. Thevenin, A. Alcalde, L.J. Pettersson, S.G. Jaras, J.L.G. Fierro, Catalytic combustion of methane over cerium-doped palladium catalysts, *J. Catal.* 215 (2003) 78–86.
- [19] P.P. Silva, F.A. Silva, H.P. Souza, A.G. Lobo, L.V. Mattos, F.B. Noronha, C.E. Hori, Partial oxidation of methane using Pt/CeZrO₂/Al₂O₃ catalysts-effect of preparation methods, *Catal. Today* 101 (2005) 31–37.
- [20] X.F. Chu, T.Y. Chen, W.B. Zhang, B.Q. Zheng, H.F. Shui, Investigation on formaldehyde gas sensor with ZnO thick film prepared through microwave heating method, *Sens. Actuators B: Chem.* 142 (2009) 49–54.
- [21] A. Forleo, L. Francioso, S. Capone, P. Siciliano, P. Lommens, Z. Hens, Synthesis and gas sensing properties of ZnO quantum dots, *Sens. Actuators B: Chem.* 146 (2010) 111–115.
- [22] T.T. Trinh, N.H. Tu, H.H. Le, K.Y. Ryu, K.B. Le, K. Pillai, J. Yi, Improving the ethanol sensing of ZnO nano-particle thin films – the correlation between the grain size and the sensing mechanism, *Sens. Actuators B: Chem.* 152 (2011) 73–81.
- [23] P.X. Gao, Y. Ding, Z.L. Wang, Crystallographic orientation-aligned ZnO nanorods grown by a tin catalyst, *Nano. Lett.* 3 (2003) 1315–1320.
- [24] N. Zhang, R. Yi, R. Shi, G. Gao, G. Chen, X. Liu, Novel rose-like ZnO nanoflowers synthesized by chemical vapor deposition, *Mater. Lett.* 63 (2009) 496–499.
- [25] R. Noriega, J. Rivnay, L. Goris, D. Kälblein, H. Klauk, K. Kern, L.M. Thompson, A.C. Palke, J.F. Stebbins, J.R. Jokisaari, G. Kusinski, A. Salleo, Probing the electrical properties of highly-doped Al:ZnO nanowire, *J. Appl. Phys.* 107 (2010) 074312.
- [26] O. Lupan, V.V. Ursaki, G. Chai, L. Chow, G.A. Emelchenko, I.M. Tiginyanu, A.N. Gruzintsev, A.N. Redkin, Selective hydrogen gas nanosensor using individual ZnO nanowire with fast response at room temperature, *Sens. Actuators B: Chem.* 144 (2010) 56–66.
- [27] R.L. Penn, J.F. Banfield, Imperfect oriented attachment: dislocation generation in defect-free nanocrystals, *Science* 281 (1998) 969–971.
- [28] Y. Wang, M.M. Tong, D. Zhang, Z. Gao, Improving the performance of catalytic combustion type methane gas sensors using nanostructure elements doped with rare earth cocatalysts, *Sensors* 11 (2011) 19–31.
- [29] L. Xu, T. Li, X.L. Gao, Y.L. Wang, Behaviour of a catalytic combustion methane gas sensor working on pulse mode, *IEEE Sensors* (2010) 391–394.
- [30] P.T. Moseley, Solid state gas sensors, *Meas. Sci. Technol.* 8 (1997) 223–237.
- [31] M.M. Tong, Analysis of two methods detecting methane with constant voltage on sensor or compensating element, *J. Chin. Univ. Min. Technol.* 31 (2002) 190–193 (In Chinese).
- [32] X.W. Ren, Z.Z. Xu, B. Zhou, Effect of catalytic carrier adulation on catalytic sensor stability, *Transducer Microsyst. Technol.* 28 (2009) 30–32 (In Chinese).
- [33] J.Z. Liu, J. Fan, X.G. Wang, Study on the catalyst combustion of CH₄ and the stability of CH₄ sensor, *Coal Convers.* 21 (1998) 87–90 (In Chinese).
- [34] H.P. Choo, K.Y. Liew, H. Liu, Factors affecting the size of polymer stabilized Pd nanoparticles, *J. Mater. Chem.* 12 (2002) 934–937.

Biographies

Fengmin Liu received the BE degree in Department of Electronic Science and Technology in 2000. She received her Doctor's degree in College of Electronic Science and Engineering at Jilin University in 2005. Now she is an associate professor in Jilin University, China. Her current research is preparation and application of semiconductor oxide, especial in gas sensor and solar cell.

Yiqun Zhang received the BE degree in Department of Electronic Sciences and Technology in 2009. She is currently studying for her ME Sci degree in College of Electronic Science and Engineering, Jilin University, China.

Yingshuo Yu received the BE degree in Department of Micro-Electronics in 2010. She is currently studying for her ME Sci degree in College of Electronic Science and Engineering, Jilin University, China.

Jing Xu received the BE degree in Department of Electronic Sciences and Technology in 2010. She is currently studying for her ME Sci degree in College of Electronic Science and Engineering, Jilin University, China.

Jianbo Sun received the BE degree in Department of Electronic Sciences and Technology in 2004. He is currently studying for his Dr. Sci degree in College of Electronic Science and Engineering, Jilin University, China.

Geyu Lu received the B.Sc. degree in Electronic Sciences in 1985 and the M.Sc. degree in 1988 from Jilin University in China and the Dr. Eng. degree in 1998 from Kyushu University in Japan. Now he is a professor of Jilin University, China. His current research interests include the development of chemical sensors and the application of the function materials.